Kinetics of grating inscription in DR1:DNA-CTMA thin film: experiment and semi-intercalation approach

G. Pawlik[a], W. Radosz[a], A.C. Mitus[a]
J. Mysliwiec[b], A. Miniewicz[b]
F. Kajzar[cd], I. Rau[c]
J.G. Grote[e]

[a] Institute of Physics,Wroclaw University of Technology, Wroclaw, Poland
[b] Institute of Physical and Theoretical Chemistry, Wroclaw University of Technology, 50-370 Wroclaw, Poland
[c] Faculty of Applied Chemistry and Materials Science, University Politehnica Bucharest, Bucharest, Romania
[d] Université d'Angers, Institut des Sciences et Technologies Moléculaires d'Angers, MOLTECH Anjou - UMR CNRS 6200
Equipe Interaction Moléculaire Optique non linéaire et Structuration MINOS 2, Bd Lavoisier, 49045 Angers cedex, France
[e] Air Force Research Laboratory, Wright-Patterson Air Force Base, Ohio, USA

ABSTRACT

The semi-intercalation hypothesis[1–5] which states that an azo-dye Disperse Red 1 (DR1) molecule intercalates in a specific way into a biopolymeric material made of DNA complexed with the cationic surfactant CTMA, has successfully explained the main experimental results[6] of laser dynamic inscription of diffraction gratings: short response time, low diffraction efficiency, single-exponential kinetics and flat wavelength dependence.[4] Recent experiments indicate that the inscription of the grating displays some features of non-exponential behavior. To understand this complex dynamics we characterize local environment of polymeric chains in Monte Carlo modelling by analyzing some features of local free-volume (void) distribution.

Keywords: DR1:DNA-CTMA, diffraction grating, degenerate two-wave mixing, Monte Carlo, bond-fluctuating, void

1. OUTLINE: SEMI–INTERCALATION IN DR1:DNA–CTMA

Deoxyribonucleic acid (DNA), functionalized with photoresponsive molecules, has been the subject of interest due to its potential application in NLO–effects based devices.[7–9] The nature of binding of azodyes to the DNA helix is not clear. Circular dichroism studies[10] show that the dyes can be oriented in DNA-CTMA in various ways (intercalated into the nanospaces between the base pairs or aligned by binding in the grooves of the DNA helix). Arguments against a full intercalation scenario were put up for discussion in Ref.[11] A breakthrough in experiment was made by You et al.[3] who have shown that the dye molecules do not interact directly with DNA; the DNA double helix acts rather as a template for the interaction between dye molecules and CTMA in the DNA/CTMA complex. The Authors draw the conclusion that there is no direct interaction between the DNA and dye molecules.

Dynamic holographic grating recording carried out in a degenerate two-wave mixing (DTWM) setup for DR1:DNA-CTMA thin film[6] showed that the dynamic holographic gratings were characterized by very short operational times (inscription/erasure), single-exponential kinetics, small diffraction efficiency, weak dependence on wavelength and optical stability and reversibility. To model those effects we have proposed a simple semi-intercalation model for photo-isomerizable dyes in a DNA polymer matrix,[1, 2, 4, 5] which mimics the inscription/erasure of diffraction gratings in DNA-CTMA polymer with an azodye, and have studied it using Monte

Carlo (MC) simulation method,[12–15] see Sect. 2.2. We have found that the dynamics of grating inscription is rather complex.

The aim of this paper is to discuss this complex dynamics, both experimentally and on a modelling level, using the characterization of local free volume close to polymeric chains.

2. SEMI-INTERCALATION MODEL: CONCEPTS, MONTE CARLO SIMULATIONS AND EARLIER EXPERIMENTS

The main assumption of the semi-intercalation model is that the dye molecule is only partially intercalated in the DNA-CTMA system. After a full photo-isomerization cycle $trans \rightarrow cis \rightarrow trans$ each molecule returns to the $trans$ form at initial orientation. The main difference between semi-intercalation model and host-guest model studied earlier[12, 13] is the absence of orientational redistribution and diffusion in the former.

2.1 Monte Carlo modelling

The Monte Carlo model of diffraction grating inscription and erasure was formulated in terms of transition probabilities (per unit of time) for photo-isomerization reactions $trans \leftrightarrow cis$ of photochromic molecules in a polymer matrix. We follow the presentation given in paper;[1] more information can be found in Ref.[17] The transition probabilities read:[12, 13]

$$p(trans \rightarrow cis) = V \, I \, p_{tc} \, \cos^2 \theta, \tag{1}$$

$$p(cis \rightarrow trans) = V \, I \, p_{ct}, \tag{2}$$

where V denotes a local (in a close vicinity of a photochromic molecule) void (free volume), see Sect. 4.1, I - light intensity, θ - an angle the long axis of the molecule makes with the polarization direction of the light, and p_{tc}, p_{ct} denote the probability of a photo-isomerization in a single act of interaction with light. We define parameter $R = \frac{p_{tc}}{p_{ct}}$ which is related to the ratio of products of absorbances and quantum yields for transitions $trans \rightarrow cis$ and $cis \rightarrow trans$. In DTWM experiments the intensity of linearly polarized light along z-direction, propagating in the y-direction, varies along x-axis: $I(x) = \frac{1}{2}(1 + \sin(qx + \pi))$ where q stands for the wave-vector of optical grating. The metod of calculation of diffraction efficiency $\eta \propto \Delta^2$ from Monte Carlo data can be found in Ref.[12]

2.2 Semi-intercalation model and experiment

The original semi-intercalation model[1] was generalized to include the polymer chain into MC modelling by taking into account the parameter V, calculated from actual MC simulations, in transition probabilities (1) and (2). Fig. 1 shows the results of the simulations[4] and compares MC kinetics of diffraction efficiency Δ^2 calculated in semi-intercalation model (lower curve) and in host-guest model (upper curve), simulated at temperature close to the glass point ($T = 0.3 \simeq T_g$), using $p_{ct} = 10^{-3}$ and real experiment for grating inscription kinetics in DR1:DNA-CTMA. Parameter R was estimated to be close to 0.3 in the range of wavelength 460 nm - 540 nm. Results of Monte Carlo simulations[4] reproduce in a satisfactory way the experimental results for DR1:DNA-CTMA system: short response time, low diffraction efficiency, nearly single-exponential kinetics and flat wavelength dependence.

Experimental data[6] for the time dependence of diffraction efficiency seem to be consistent with a single exponential inscription. Our simple analytic model[4, 5] offers a more complicated physical picture, where single-exponential behaviour is a limiting case corresponding to $R \rightarrow 0$. For non-zero values of R the model kinetics becomes non-exponential. This behaviour can be related to a set of relaxation times which contribute with unknown weights to the dynamics of the inscription. In Section 4 we discuss a hypothetical origin of this behaviour, closely related to distribution of voids in the system.
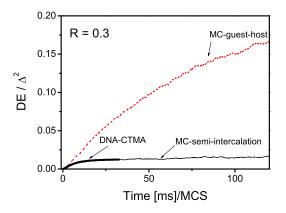
Figure 1. Monte Carlo simulations of inscription of diffraction grating for $R = 0.3$. $T = 0.3 \simeq T_g, p_{ct} = 10^{-3}$ in guest–host and semi–intercalation models and results of a DTWM experiment for the kinetics of grating inscription in DR1:DNA-CTMA system. After Ref.[4]

3. NEW EXPERIMENTAL RESULTS

We have repeated standard DTWM experiments[4,6] with grating inscription in DR1:DNA-CTMA in a slightly changed setup. This time the gratings were written on a freshly prepared sample using two beams from the start. Moreover, much longer measurements were taken. Fig. 2 shows the time-dependence of intensity measured in the first diffraction peak, with two fits: stretched exponential (left) and bi-exponential (right). The former is clearly unsatisfactory, the latter is not good. We conclude that the inscription of the grating using present setup does not follow a single exponential pattern. For comparison with a standard host-guest system we have done similar experiments using DR1:PS system. The results are shown in Fig. 3. While the temporal inscription pattern is different than for DR1:DNA-CTMA system (in agreement with Ref.[4]) stretched exponential and bi-exponential fits are worse than for DR1:DNA-CTMA case. We conclude that the mechanisms responsible for the inscription of the gratings are different in both cases. In our opinion an origin of this difference can be related to various distributions of local voids in both systems. Thus, the study of this topic becomes a challenge. In the next Section we present some preliminary results on this topic.
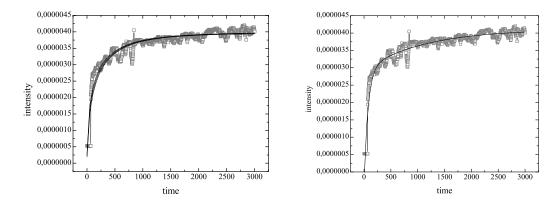

Figure 2. Time evolution of measured intensity (in W) for DR1:DNA-CTMA system. Time unit: 100 ms. Solid line are fits: stretched exponential (left) and bi-exponential (right).
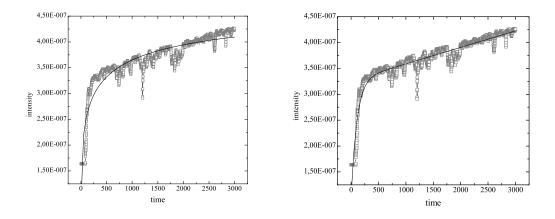
Figure 3. Time evolution of measured intensity (in W) for DR1:PS system. Time unit: 100 ms. Solid line are fits: stretched exponential (left) and bi-exponential (right).

4. MODEL OF DR1:DNA-CTMA REVISITED

4.1 Voids in bond-fluctuating model[5]

The voids (local free volumes) in a polymer matrix play a decisive role for its dynamics as well as for the dynamics (kinetics) of orientations of guest molecules. In our approach the polymer matrix was simulated using bond-fluctuating Monte Carlo method in 3D.[16] Six non-equivalent bond orientations were used, with lengths (in lattice constants): 2, $\sqrt{5}$, $\sqrt{6}$, 3, 3, $\sqrt{10}$. The corresponding dimensionless energy values were equal 1 for the first three cases, and 0 for the last three lengths. $N = 24000$ polymer chains, each consisting of $L = 20$ monomers, were placed on a $V_p = 200 \times 200 \times 200$ lattice, which yields the reduced density $\rho = 8\,N\,L/V_p = 0.48$. The simulations were made at constant reduced temperature $T = 0.3$ (temperature unit is related to energy scale introduced by bond energy); the glass temperature reads approximately $T_g \approx 0.28$. Initial configuration consisted of isotropically oriented dyes. More details can be found in Refs.[13–15]
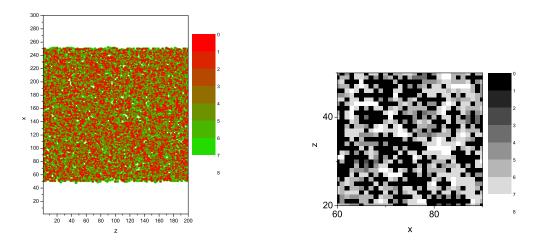

Figure 4. Snapshots: spatial distribution of void parameter V in $x - z$ plane. After Ref.[4]

The void parameter V, which characterizes the size of local free volume around each lattice site, is calculated

on the basis of an occupancy of $3 \times 3 \times 3$ neighboring cubes. If no monomers are present in this neighborhood then $V = V_0 = 7$. If a monomer occupies the central site or one of its 6 nearest neighbors (along x, y, z axes) then $V = 0$. Each monomer within the cube (excluding the 7 positions just discussed) decreases the value of parameter V by 1. The choice of assigned values (V_0) is arbitrary. In two–dimensional case this arbitrariness leads to a redefinition of the viscosity of the polymeric matrix. For more details see.[17] An exemplary spatial distribution of parameter V in $x - z$ plane is presented in Fig. 4. A quick inspection reveals a rather complex distribution of free (large values of V) and occupied (small values of V) areas, which hinder the DR1 kinetics in different ways.

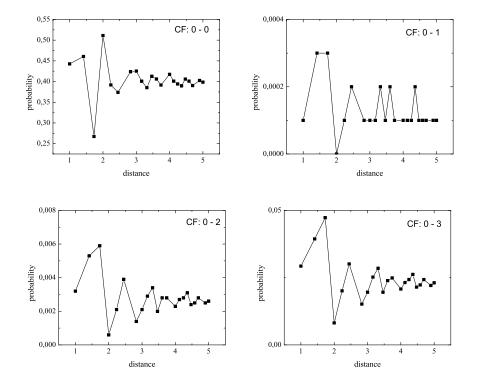## 4.2 Characterization of voids close to polymeric chains

Figure 5. Plots of correlation functions $g_2(r, V, 0)$, $V = 0, 1, 2, 3$.

To study the distribution of voids close to the polymeric chain we use a correlation function $g_2(r, V, V_0)$ which is the conditional probability to find a cell with void characteristic V at distance r from a cell with void characteristic V_0. It constitutes a straightforward generalization of radial distribution function $g_2(r)$ in the theory of liquids. Figs. 5 and 6 show the plots of $g_2(r, V, 0)$, which characterize the correlations in the spatial distribution of local voids at distance r from a cell with a maximum of steric hindrances ($V = 0$). Approximately 15% of cells with $V = 0$ is occupied by monomers. All the plots display oscillations typical for simple liquids. The plots for voids with small amount of steric interactions, $V = 6, 7$ are different than the remaining plots - they show a clear tendency for a separation from cells with strong steric hindrances. This proves that the distribution of voids in space is not fully random and that the correlations are clearly present. The nature of those correlations requires further studies.[18]

The distribution of cells with weak and strong steric interactions close to the polymeric chain can be easily illustrated. Fig. 7 shows a chosen polymeric chain with its nearest neighborhood (distance 1) corresponding to $V = 0$ (grey) and $V = 6$ (dark). Clearly, the number of former is substantially larger than of the latter. This observation suggests that a polymeric chain is wrapped up with a kind of a tube which promotes strong steric interactions.[18]
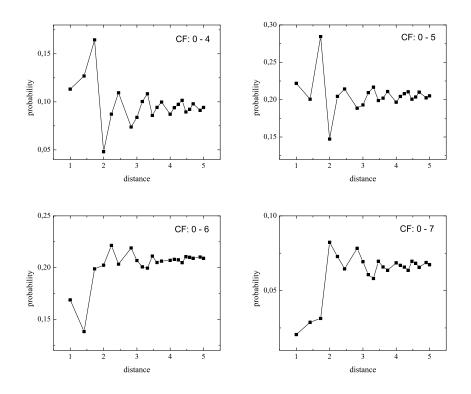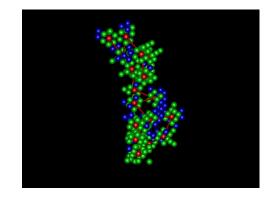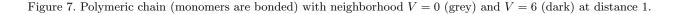
Figure 6. Plots of correlation functions $g_2(r,,V)$, $V = 4, 5, 6, 7$.

Figure 7. Polymeric chain (monomers are bonded) with neighborhood $V = 0$ (grey) and $V = 6$ (dark) at distance 1.

5. DISCUSSION

We have shown that the inscription of diffraction gratings in DR1:DNA-CTMA and DR1:PS systems is non-exponential on a long time scale. We assign this complex behaviour to inhomogeneities in the distribution of local free volume (voids) in the polymeric matrix. Using bond-fluctuating Monte Carlo approach, we have studies some features of spatial distribution of voids with strong and weak steric hindrances. We have shown that this distribution is not homogeneous and that close to polymeric chains steric interactions are strong. Further studies, in particular those of the distributions of sizes of various voids, are necessary for an explanation of non-exponential kinetics of inscription of diffraction gratings.

Acknowledgements

REFERENCES

1. A.C. Mitus, G. Pawlik, A. Kochalska, J. Mysliwiec, A. Miniewicz, and F. Kajzar, Proc. SPIE **6646**, 66460I (2007).
2. A.C. Mitus, G. Pawlik, F. Kajzar, and J.G. Grote, Proc. SPIE **7040**, 70400A (2008).
3. H. You, H. Spaeth, V.N.L. Linhard, and A.J. Steckl, Langmuir **25**, 11698 (2009).
4. G. Pawlik, A.C. Mitus, J. Mysliwiec, A. Miniewicz, and J.G. Grote, Chem. Phys. Lett. **484**, 321 (2010); Proc. SPIE **7765**, 776504 (2010).
5. A.C. Mitus, G. Pawlik, W. Kordas, J. Mysliwiec, A. Miniewicz, F. Kajzar, I. Rau, and J.G. Grote, Proc. SPIE **8103**, 810309 (2011).
6. A. Miniewicz, A. Kochalska, J. Mysliwiec, A. Samoc, M. Samoc, and J.G. Grote, Appl. Phys. Lett. **91**, 04118 (2007).
7. E. M. Heckman, J.A. Hagen, P.P. Yaney, J.G. Grote, and F.K. Hopkins, Appl. Phys. Lett. **87** 211115 (2005).
8. A. Samoc, M. Samoc, A. Miniewicz, J.G. Grote, and B. Luther-Davies, Proc. SPIE **6401**, 640106 (2006).
9. A. Samoc, A. Miniewicz, M. Samoc, and J.G. Grote, J. Appl. Polym. Sci. **105** 236 (2007).
10. G. Zhang, H. Takahashi, L. Wang, J. Yoshida, S. Kobayashi, S. Horinouchi, and N. Ogata, Proc. SPIE **4905**, 375 (2002).
11. M. Samoc, A. Samoc, A. Miniewicz, P.P. Markiowicz, P.N. Prasad, and J.G. Grote, Proc. SPIE **6646**, 66460A (2007).
12. G. Pawlik, A.C. Mitus, A. Miniewicz, and F. Kajzar, J. Chem. Phys. **119**, 6789 (2003).
13. G. Pawlik, A.C. Mitus, A. Miniewicz, and F. Kajzar, J. Non. Opt. Phys. & Mat. **13**, 481 (2004).
14. G. Pawlik, A. C. Mitus, A. Miniewicz, and F. Kajzar, Nonl. Opt. & Quant. Opt. **35**, 21 (2006).
15. G. Pawlik, A.C. Mitus, and F. Kajzar, Proc. SPIE **6330**, 633003 (2006).
16. H. P. Deutsch, and K. Binder, J. Chem. Phys. **94**, 2294 (1991).
17. G. Pawlik, A.C. Mitus, I. Rau, and F. Kajzar, Nonl. Opt. Quant. Opt. **38**, 227 (2009).
18. G. Pawlik, R. Orlik, W. Radosz, A.C. Mitus, and M.G. Kuzyk, Proc. SPIE **8474**, (2012), submitted.